DOI 10.1007/s10008-006-0161-8

Polypyrrole-Fe_2O_3 nanohybrid materials for electrochemical storage

M. Mallouki · F. Tran-Van · C. Sarrazin · P. Simon · B. Daffos · A. De · C. Chevrot · J. Fauvarque

Abstract We report on the synthesis and electrochemical characterization of nanohybrid polypyrrole (PPy) (PPy/Fe_2O_3) materials for electrochemical storage applications. We have shown that the incorporation of nanoparticles inside the PPy notably increases the charge storage capability in comparison to the "pure" conducting polymer. Incorporation of large anions, i.e., paratoluenesulfonate, allows a further improvement in the capacity. These charge storage modifications have been attributed to the morphology of the composite in which the particle sizes and the specific surface area are modified with the incorporation of nanoparticles. High capacity and stability have been obtained in PC/NEt_4BF_4 (at 20 mV/s), i.e., 47 mAh/g, with only a 3% charge loss after one thousand cyles. The kinetics of charge–discharge is also improved by the hybrid nanocomposite morphology modifications, which increase the rate of insertion–expulsion of counter anions in the bulk of the film. A room temperature ionic liquid such as imidazolium trifluoromethanesulfonimide seems to be a promising electrolyte because it further increases the capacity up to 53 mAh/g with a high stability during charge–discharge processes.

Keywords Nanocomposites · Conducting polymers · Electrochemical storage · Room temperature ionic liquid

M. Mallouki · F. Tran-Van · C. Sarrazin · C. Chevrot (✉)
Laboratoire de Physicochimie des Polymères et des Interfaces,
LPPI, EA 2528 Université de Cergy-Pontoise 5,
mail Gay-Lussac,
95031 Cergy-Pontoise Cedex, France
e-mail: claude.chevrot@chim.u-cergy.fr

J. Fauvarque
Laboratoire d'Electrochimie Industrielle, CNAM,
75003 Paris, France

P. Simon · B. Daffos
Université Paul Sabatier,
CIRIMAT-LCMIE, UMR 5085, 118 route de Narbonne,
31062 Toulouse, France

A. De
Saha Institute of Nuclear Physics,
1/AF, Bidhannagar,
Calcutta 700064, India

Introduction

In the field of energy storage and conversion systems, electronically conducting polymers (ECPs) are promising materials. Their high specific capacitance and high conductivity in the charged state allow applications in electrochemical storage devices such as supercapacitors or batteries [1–3]. Unlike double-layer capacitors, in which the energy storage is electrostatic in origin, ECPs are pseudocapacitor materials with faradaic processes due to reversible electrochemical doping–dedoping reactions. Thus, ECPs can be interesting materials for increasing the charge storage capacity in comparison with double-layer activated carbons. Furthermore, the processability of these materials for building well-adapted electrodes for storage devices has been shown [4]. Depending on the configuration of the cell, different classes of ECP-based supercapacitors have been described [1]. Type 1 supercapacitors use one p dopable conjugated polymer as both the anode and cathode of the device. In type 2 supercapacitors, two different p dopable ECPs are used that have different ranges of potential for oxidation. Finally, type 3 supercapacitors can be obtained by the combination of one n and p dopable ECP, which ensures a high potential in the charged state and allows the performance of the cell to be increased. Nevertheless, the stability of the n doped ECP still needs to be improved to increase the lifetime of such a

configuration. More recently, hybrid cells using activated carbon as a negative electrode and ECP as a positive one have been suggested as an alternative to all polymer devices [4]. Among conducting polymers, polypyrrole (PPy) is particularly attractive because of its low cost and its good electrochemical stability.

For supercapacitor applications, conducting polymers deposited on activated carbons have been suggested to increase the charge storage properties [5–7]. Recently, nanotubular composites of carbon nanotubes and conducting polymers have been studied for supercapacitor applications [8–13]. Taking into account the high cost of carbon nanotubes, it could be interesting to study an alternative route for the preparation of hybrid materials for energy storage.

Concerning organic/inorganic hybrid electrodes, the combination of conducting polymers and inorganic nanoscaled species to form nanocomposite hybrid materials could represent an opportunity for the design of materials with improved properties, such as charge storage capabilities, stability during cycling, and dynamics of charge propagation. Depending on the nature of the inorganic partner, two main groups of hybrid electrode materials can be defined: intercalative nanocomposites containing, for example, FeOCl, V_2O_5, $RuCl_3$, Clays... [14–19], in which polymerization is carried out inside a layered or 3D structure, and inorganic-incorporated nanocomposites, in which the oxide particles act as a high-surface-area colloidal substrate for the polymerization of conjugated organic materials [21, 22]. Concerning intercalative nanocomposites, different groups have studied the possibility of using nanohybrid structures to increase the electrochemical storage properties [19–23].

In the field of inorganic-incorporated nanocomposites, different PPy-based nanostructures containing iron nanoparticles (Fe_3O_4, Fe_2O_3, and $CoFe_2O_4$) have already been synthesized, and their physical properties have been characterized [24–34]. Other oxide nanoparticles, such as Al_2O_3, TiO_2, ZrO_2, and SiO_2, have also been incorporated into ECPs. [35–38]. Due to the easy preparation and the good stability of the colloidal Fe_2O_3 solution, as well as the simple chemical synthesis of the nanohybrid PPy/Fe_2O_3 materials, we have studied the possibility of modifying the nanostructure of a conducting polymer by the incorporation of nanoparticles, with the aim of increasing the electrochemical storage of the electroactive material. In this work, our aim was to study the influence of the modification of the morphology of PPy by polymerization onto nanoparticles to increase the charge storage capacity of the electroactive polymers. We will describe the preparation of PPy/Fe_2O_3 nanocomposites with different compositions of iron nanoparticles and different counter anions incorporated in the nanostructure. The morphology of the materials will be studied, and their electrochemical behavior (capacity, kinetic of charge–discharge), depending on the material's composition, will be presented. The optimum conditions for high charge storage and good capacity stability during the charge–discharge process will also be studied to optimize the performance of such materials for electrochemical storage applications.

Experimental part

Materials

Pyrrole was purchased from Aldrich and was purified by distillation under reduced pressure, and was stored at −10 °C. All other chemicals were of reagent grade and used without further purification.

Preparation of composites

PPy (sample A) was prepared by chemical polymerization of 1 g of pyrrole using 2.5 equivalent of $FeCl_3$ (6.05 g) (per mole of pyrrole) in distilled water at ~5 °C with constant stirring for 1 h. Nanocomposite PPy/Fe_2O_3 (sample B) was prepared by chemical polymerization of pyrrole in a colloidal solution of Fe_2O_3. The colloidal solution was prepared using a standard procedure as described elsewhere [39]. Of a 32-wt.% ferric chloride solution, 12 ml was poured into 750 ml of boiling water. A dark red-colored colloid was readily formed, and was then dialyzed until it was free from ions and stored. Of the colloidal solution, 50 ml was used and the volume was reduced to about 15 ml by evaporation (at 90 °C at ambient pressure). The amount of Fe_2O_3 in the colloidal solution was evaluated at 90 mg as already determined [29]. To this remaining volume, 0.25 ml of pyrrole was added under constant stirring. Then, an aqueous solution containing 2.5 equivalents of $FeCl_3$ (1.51 g) with respect to the initial amount of pyrrole was added dropwise, with continuous stirring at ~5 °C for about 1 h.

After polymerization, the resulting material precipitated out of the solution and settled down as a black solid, which was filtered, washed thoroughly with distilled water, and vacuum dried at 50 °C. The material contained 12.46% N, 15.01% Fe, and 8.53% Cl.

PPy/paratoluenesulfonate (PTS) (sample C) was prepared by chemical polymerization of 1 g of pyrrole using 2.5 equivalents of $FeCl_3$ (6.05 g) in the presence of 5.8 g of sodium-PTS as a doping agent (2 mol PTS/Py) in distilled water at ~5 °C for 1 h. After filtration, washing, and vacuum drying at 50 °C, we obtained black powder. This powder contained 10.94% N, 1.73% Fe, and 6.74% S.

PPyPTS/Fe_2O_3 nanocomposites (samples D1 to D4) were prepared by chemical polymerization of pyrrole into a colloidal solution of Fe_2O_3, as described for sample B. The

volumes of pyrrole [400 μl (sample D4), 125 μl (D3), 62 μl (D2), and 31 μl (D1)] were added under constant stirring. Then, a solution containing 2.5 equivalents of $FeCl_3$/pyrrole and 2 equivalents of PTS sodium salt/pyrrole was added dropwise, with continuous stirring at ~5 °C for about 1 h. Black powders were filtrated, washed, and dried at 50 °C under vacuum. Sample D1 contained 6.24% N, 31.13% Fe, and 4.22% Cl; sample D2 contained 8.71% N, 20.49% Fe, and 3.04% Cl; sample D3 contained 9.41% N, 14.84% Fe, and 2.84% Cl; and sample D4 contained 10.68% N, 9.10% Fe, and 3.51% Cl. Nanocomposite with naphthalene sulfonate ($PPyNS/Fe_2O_3$) and anthraquinone disulfonate ($PPyAQDS/Fe_2O_3$) was also prepared with a similar procedure and the same initial proportion of each reagent as that of sample D4.

Room temperature ionic liquid (RTIL)

1-Ethyl-3-methylimidazolium bis((trifluoromethyl)sulfonyl) imide (EMITFSI) was synthesized as described by Bonhôte et al. [40], starting from 1-methylimidazole (Aldrich 99%), bromoethane (Aldrich 98%), and lithium trifluoromethanesulfonimide (Aldrich 99.5%).

Processing

The electrochemical tests were performed on composite polymer electrodes; the electrodes were made up of an active material laminated onto expanded metallic current collectors. To prepare the active material, the polymer powder was mixed together with an electronic conductive powder (acetylene black: Alfa Cesar) to enhance the polymer's electronic conductivity. An organic binder was then added to the mixture to improve mechanical properties.

To better characterize the PPy/Fe_2O_3 nanocomposites, we chose to introduce high contents of electronic conducting particles (acetylene black). In this case, the composite electrode is not optimized for supercapacitor application, but such a composition is well adapted for a good characterization of the conducting polymer. Indeed, the ohmic drop is low, favoring the electronic transfer inside the composite electrode. Thus, the working electrode was mainly prepared by mixing 30 wt.% of active material, 65 wt.% of acetylene black, and 5 wt.% of binders (3 wt.% of carboxymethylcellulose and 2 wt.% of polytetrafluoroethylene) to make a paste, which was then laminated onto a 1-cm^2 expanded stainless steel grid (AISI 316L), as previously described [41].

The counter electrode (CE) was made out of activated carbon (PICACTIF, PICA) (95, 5 wt.% of binder), bound on an expanded stainless steel grid (4 cm^2). The capacity of the CE (12 F) was about five times higher than that of the working electrode to limit potential shifting by avoiding the degradation of electrolytes on the CE.

The reference electrode was Ag^+/Ag 10^{-2} M in acetonitrile for studies carried out in organic electrolytes and in ionic liquid. The potential of this reference electrode is +0.29 V/saturated calomel electrode (SCE). In aqueous media, we used SCE as the reference electrode. The capacity was determined per gram of nanocomposite (PPy/Fe_2O_3), in the case of the nanohybrid materials, and per gram of PPy, in the case of the pure conductive polymer (taking into account the weight of the PTS counter anions).

Apparatus

A Biologic versatile multipotentiostat was used for potentiodynamic and galvanostatic measurements. Electronic conductivity was determined with a four-probe apparatus (Jandel). Adsorption and desorption isotherms for nitrogen were obtained at 77 K using a COULTER S 3100 apparatus. The samples were out-gassed at 373 K and 0.1 Pa for 2 h before measurements. Specific surface area values were computed using the Brunauer–Emmett–Teller (BET) equations.

Results and discussion

Influence of the iron nanoparticles on the charge storage capacity

The main objective of this work was to optimize the capacity of chemically synthesized PPy, as well as its stability during cycling. Ko and coworkers [42] have recently shown the important effect of the solvent used in the chemical polymerization of pyrrole on the electrochemical pseudocapacitance properties of the materials. The best results were obtained in the aqueous media in which the morphology of the polymer appeared to be the most porous [42]. To increase the electrochemical capacity of the chemically synthesized PPy, we first carried out the synthesis of a PPy/Fe_2O_3 nanocomposite from polymerization of pyrrole in an aqueous colloidal solution containing iron oxide particles. The colloid particles are polydisperse spheres lying in the size range from 25 to 50 nm. After composite formation, these particles are found to be entrapped within PPy chains [43]. The colloidal particles act here as a support to the growing polymer chains.

Figure 1a shows the evolution of the current/gram of electroactive material (PPy or hybrid material + counter anion) during potential scans and indicates that the intensity of the signal is increased in the presence of inorganic iron oxide particles (Fig. 1a, samples A and B). The charge storage capability is increased by 22% compared with pure

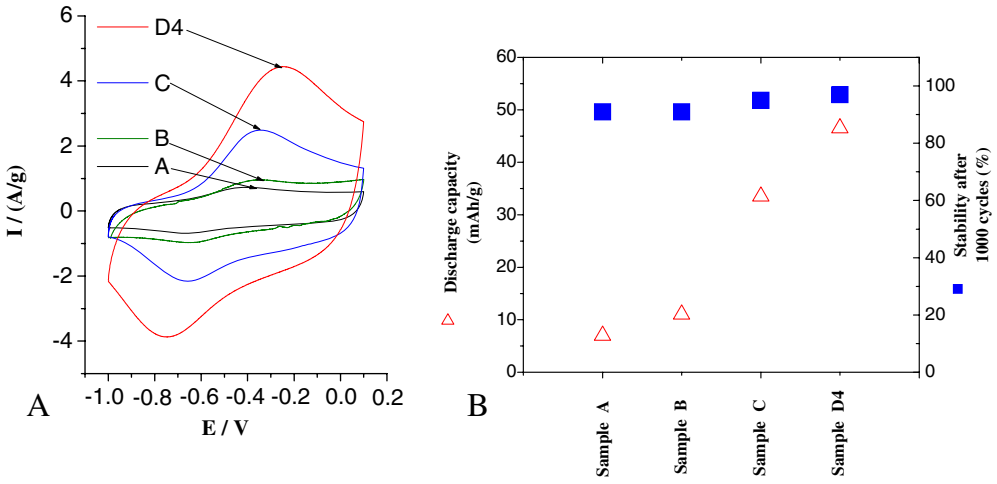

Fig. 1 Cyclic voltamograms at 20 mV/s (**a**) and maximum capacity and stability after 1,000 potentiodynamic cycles between −1 and 0.1 V (**b**) for PPy (sample A), PPy/Fe_2O_3 (sample B), PPy/PTS (sample C), and PPyPTS/Fe_2O_3 (sample D4), in PC/1 M NEt_4BF_4

PPy, but remains rather low (less than 12 mAh/g) (Fig. 1b, samples A and B).

Influence of large anions size-synergy of the charge storage properties

The polymerization of conducting polymers with surfactant anions acting as permanent doping agents immobilized in the polymer matrix has been studied by different groups [44–47]. The subsequent process of doping can proceed by the ejection of cations followed by the insertion of additional anions from the electrolyte solution. In the case of an electrolyte with cations moving faster than anions, the kinetics of charge transfer could be improved and specific power could be increased. Moreover, the morphology of the polymeric material can be strongly influenced by the nature of the counter ion. The concept of ladder-doped polymer as an electrode in high-power electrochemical supercapacitors has been proposed by Ingram and coworkers [45]. In their work, sulfonic and disulfonic counter ions were investigated to ensure an anionic bridge between conducting oxidized polymeric chains, as well as a more open structure with channels in which fast ionic motions can occur. In accordance with this concept, we included different large anions (PTS, naphtalenesulfonate, and anthraquinonedisulfonate) during the synthesis of the nanohybrid structure to enhance the performance of the nanocomposite materials. Table 1 shows the influence of the anion nature on the specific capacity of the materials. The best results in terms of capacity and stability were obtained with PTS. These results could be explained by a good compromise between the anion size that opens the structure of the composite and its relatively low molecular weight compared to the other large anions. Therefore, we used PTS as doping agent in the following part of the study.

Table 1 Evolution of the specific capacity for different doping species

Samples	PPyPTS/Fe_2O_3 (sampleD4)	PPyAQDS/Fe_2O_3	PPyNS/Fe_2O_3
Discharge capacity (mAh/g)	47	32	17
Stability of the capacity after 1,000 cycles (%)	97	90	92

Figure 1a,b (sample C) shows clearly that the addition of PTS ions improves the charge storage capacity of the PPy. Indeed, the capacity increases from 9 to 33 mAh/g by the modification of the counter anions ($FeCl_4^-$ or PTS). Moreover, the preparation of nanocomposite including iron oxide particles doped with PTS allows the further increasing of this capacity (Fig. 1a,b sample D4), which indicates a synergy of the electrochemical storage properties due to the concomitant incorporation of PTS and iron nanoparticles.

The capacity obtained with a PTS-doped nanocomposite (PPyPTS/Fe_2O_3) reaches 47 mAh/g in 1 M NEt_4BF_4 propylene carbonate solution at a scan rate of 20 mV/s. This corresponds to an increase of 28% compared to the similar non-nanostructured PPy (PPyPTS) in the same experimental conditions. This improvement could be due to an increase of the accessibility of PPy inside the electrode when this electrode is nanostructured. This nanohybrid material could lead to a more open structure, emphasized by large anions.

It is noteworthy that the iron oxide nanoparticles alone did not show specific electroactive characteristics in the range of the potentials studied. The improvement of the electrode performance compared to the electrode without particles would probably be due to the morphology modification of the conducting chains. Moreover, the electrochemical stability of the composite electrodes is quite good for a charge–discharge process limited to −1 and 0.1 V/Ag:Ag^+, because only 3% of the capacity is lost after one thousand cycles (Table 2). When the charge or the

Table 2 Influence of the limit potentials on the capacity (at 20 mV/s) and on the capacity stability during the charge–discharge process for sample D4

Voltage [V/(Ag/Ag$^+$)]	Discharge capacity (mAh/g)	Stability after 1,000 cycles (%)
−1↔0.1	47	97
−1↔0.3	54	89
−1↔0.5	65	80
−1.2↔0.1	55	88
−1.5↔0.1	60	83

discharge of the material is too deep, i.e., if the limits of potential increase (upper potential higher than 0.1 V/Ag:Ag$^+$ and/or lower potential lower than −1 V/Ag:Ag$^+$), we clearly see an important decrease of the electrochemical stability after 1,000 cycles.

Electrochemical behavior of nanocomposites—influence of the relative composition PPy/Fe_2O_3

We have studied the influence of the PPy fraction in a nanocomposite with Fe-oxide to optimize the performance of the nanocomposite electrodes for electrochemical storage. The proportion of each component was evaluated by elemental analysis from the determination of the weight percentage of nitrogen atoms (corresponding to pyrrole), iron (for Fe_2O_3+$FeCl_4^-$), and chlorine (for $FeCl_4^-$). We have already shown that the conductivity of similar nanocomposite materials is strongly influenced by the proportion of PPy [29]. Figure 2 shows the conductivity and capacity change of the composites (containing PTS) for different ratios of PPy/Fe_2O_3 (determined from elemental analysis). We obtained a maximum of conductivity with a composition of 70 wt.% of conducting polymer. The conductivity of nanocomposites can reach 57 S/cm, although the conductivity of PPyPTS is limited to 8 S/cm. This increase of electronic conductivity is interesting to limit the ohmic drop within the electrode and to allow for an increase of the active conducting composite proportion vs carbon particles. For a high proportion of inorganic particles, a drop of conductivity is observed due to the lower conductivity of pure Fe_2O_3 (0.06 S/cm) by comparison with the doped PPy. Figure 2 also indicates the evolution of the charge storage capacity vs the proportion of Fe_2O_3 particles. A maximum is obtained for a relative composition in the range of 70–82% of PPy in the nanocomposite. We clearly observe a synergy of the electrochemical storage properties for the nanohybrid composite's properties due to the association of the nanoparticles and the electroactive material.

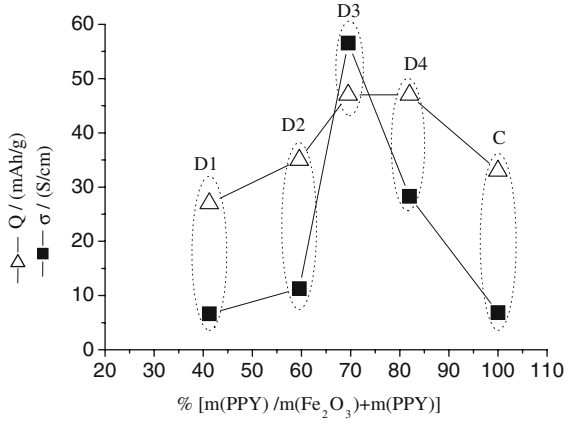

Fig. 2 Evolution of the conductivity (*square*) and capacity (*triangle*) for different relative compositions in the composite PPyPTS/Fe_2O_3 (samples D1 to D4 and C)

Figure 3a shows the evolution of the charge storage capacity of PPyPTS (sample C) and of the nanocomposite D3 for different charge–discharge currents. It is clear that even for slow doping–undoping processes (1 mA/cm^2), the capacity is much higher for the PPyPTS/Fe_2O_3 nanocomposite than for PPyPTS. Therefore, the increase of the charge storage capacity for the nanocomposite cannot be explained exclusively by a kinetic aspect, but is also an intrinsic characteristic of the material. The evolution of the specific capacity ratio Q(D3)/Q(C) for different discharge currents indicates a large increase at high current density (Fig. 3b). This indicates an improvement of the capacity of the nanocomposite, which ensures high capacity even for an important discharge current. This is particularly interesting for supercapacitor applications for which the specific power is a key parameter.

The morphology of the nanostructured PPyPTS/Fe_2O_3 was studied by scanning electron microscopy (Fig. 4). We can observe some more or less spherical particles corresponding to the conducting polymer, in which colloidal ferric oxide acts as a support to the growing polymer chains. The distribution of the particle sizes is evaluated in the range of 400–500 nm, smaller than the sizes of the particles obtained in the same conditions but without colloidal particles (larger than 1 μm).

BET measurements were also carried out to study the evolution of the specific surface area of the different samples (Table 3). For PPyPTS, a value of 12 m^2/g was obtained, in agreement with the literature [35]. When the nanoparticles were included in the material, the specific surfaces of the composites reached 44 and 45 m^2/g for samples D4 and D3, respectively. The presence of particles during the polymerization would decrease the interchain interactions and the compacity of the structure, compared to PPyPTS. When the ratio of iron particles is too high in the nanocomposites (60–40 wt.% Fe_2O_3/PPy), the specific surface area of the composite drops to 25 m^2/g and is attributed to the aggregation of the iron oxide particles.

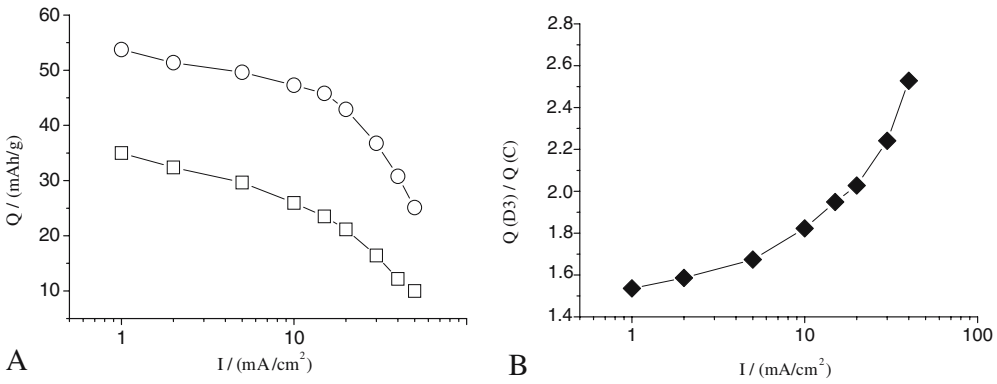

Fig. 3 Evolution of the capacity vs discharge current for $PPyPTS/Fe_2O_3$ (sample D3) (*circle*) and PPyPTS (sample C) (*square*) (**a**) and evolution of the ratio Q(D3)/Q(C) for different discharge currents (**b**) in PC/1 M NEt_4BF_4

The large porosity of the structure obtained (sample D3) would allow a better accessibility of the electrolyte inside the bulk of the material and would lead to an increase of the capacitance.

Influence of the pore size distribution

The relation between the charge storage capacity and the pore size distribution was studied for different nanocomposites (with or without PTS) having relatively high specific surface areas (43–45 m^2/g) (samples B and D3). The pore size distributions are shown in Table 4. For sample B, the proportion of micropores (<20 nm) is quite important (more than 70%) and the proportion of macropores (>80 nm) is low. The incorporation of electrolyte inside the porous structure is probably quite difficult, which limits the electroactivity of the PPy and the capacity of the nanomaterial. For sample D3, we clearly see an increase of the relative proportion of meso and macropores in the nanostructure, which reach up to 72% of the global porosity. Moreover, the proportion of micropores (<20 nm) is low (around 27%). The accessibility inside the bulk is improved, which could explain the large improvement of the charge storage capacity of the nanocomposites incorporating PTS by comparison with the ones doped with $FeCl_4^-$.

Composition of the electrode-rate of acetylene black (electronic conductor)

The realization of electrodes with high electrochemical storage properties requires the amount of active materials to be optimized as much as possible with the amount of conducting polymer or nanocomposite. Therefore, we studied the evolution of the charge storage capacity (per gram of active materials) with the proportion of the active material, i.e., hybrid nanocomposite ($PPyPTS/Fe_2O_3$) or "pure" PPy (PPyPTS), into the electrode (containing acetylene black, polytetrafluoroethylene, carboxymethylcellulose). Figure 5a indicates that, even for high contents (80 wt.%) of nanocomposite (sample D3), the capacity is much higher than the capacity obtained with PPyPTS with the same composition (more than 2.2 times higher, according to the experimental conditions). Moreover, we observed a decrease of the capacity (per weight) when the amount of active material increased from 30 to 80%. For the electrodes containing nanocomposite materials, the charge storage capacity was constant up to 50% of active materials, and decreased by only 13% (of the initial capacity) when the nanocomposite content reached 80%. Nevertheless, the decrease was less important for the nanocomposites than for PPyPTS. Indeed, for electrodes containing PPyPTS, the capacity decreased quasilinearly

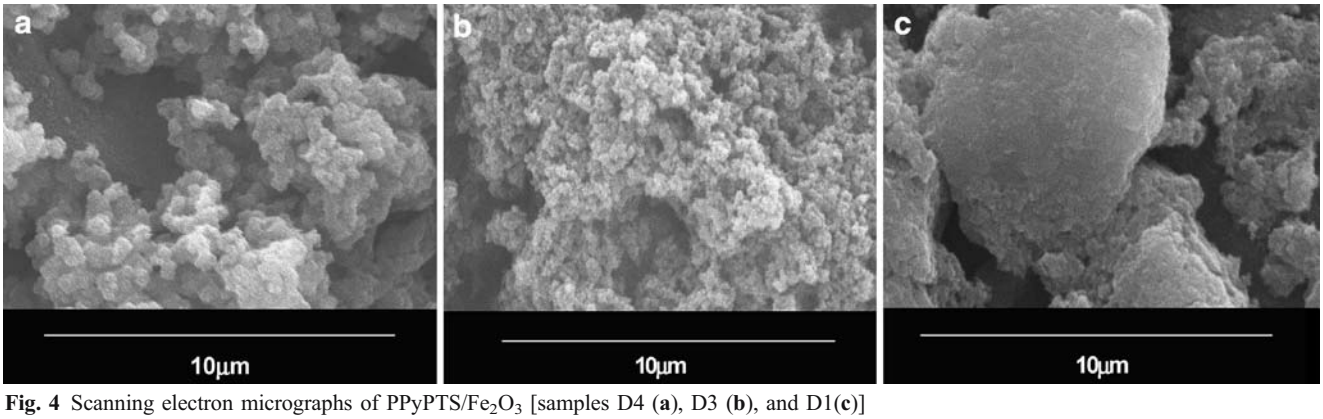

Fig. 4 Scanning electron micrographs of $PPyPTS/Fe_2O_3$ [samples D4 (**a**), D3 (**b**), and D1(**c**)]

Table 3 Influence of the composition on the physical properties and electrochemical ones

	Initial composition % (wt.%) (Py–Fe_2O_3)	Relative composition % (wt.%) (PPy–Fe_2O_3)	Conductivity (S/cm)	BET (m^2/g)	Q_{max} [mAh/g(active material)][a]
C			6.9	12	33
D4	81.63/18.37	81.82/18.18	28.3	44	47
D3	58.14/41.86	69.48/30.51	56.6	45	47
D1	25.62/74.38	41.25/58.75	6.6	24	27

[a]Obtained by cyclic voltametry at 20 mV/s in PC/1 M NEt_4BF_4 with 30 wt.% of active material in the electrode

from 34 to 21 mAh/g when the amount of PPyPTS increased from 30 to 80% of the conducting polymer (38% of charge loss).

An increase of the electronic conductivity which allows a better collection of the charge from the bulk to the electronic collector could explain the improvement of the electrochemical storage for a high amount of the active material. It is also possible that a better accessibility of the electroactive sites due to the presence of iron oxide nanoparticles improved the capacity.

In Fig. 5b, we have compared the evolution of the ratio of current density/scan rate vs voltage for the electrode containing 80 wt.% of PPy/Fe_2O_3 nanocomposites (sample D3) or PPyPTS (sample C). We clearly see during the oxidation the contribution of the faradic process (between −0.6 and −0.25 V) and the contribution of the pure capacitive process (up to −0.25 V). The large increase of the capacity for the nanocomposite (D3) by comparison with PPy is mainly due to the increase of the charge transfer properties of the nanohybrid structure. Moreover, we also observed an increase of the pure capacitive charge storage properties, which could be due to the increase of the specific surface area of the material.

Influence of the nature of the electrolyte-electrochemical behavior in room temperature ionic liquids (RTILs)

The capacity and cyclability of the PPyCPTS/Fe_2O_3 (sample D3) have been studied by repeated charge–discharge galvanostatic cycles at ±10 mA between −1.0 and 0.1 V/Ag:Ag^+ in different organic electrolytes: PC/1 M NEt_4BF_4, CH_3CN/1 M NEt_4BF_4, and EMITFSI as room temperature ionic liquid (RTIL) and between −1.0 and 0.1 V/SCE in H_2O/1 M $LiClO_4$ (Fig. 6).

In CH_3CN/1 M NEt_4BF_4, even if the maximum capacity is increased up to 55 mAh/g, the stability drops drastically to only 56% of its initial value after 1,000 cycles. In aqueous media (H_2O/1 M $LiClO_4$), we can observe a dramatic increase of the capacitance (61 mAh/g) during the first cycles. This indicates a large accessibility of the electrolyte inside the hybrid material porous nanostructure and a good impregnation of the electrolyte, allowing a fast insertion and extraction of anions during the charge–discharge process. Nevertheless, the stability is not satisfactory because a loss of 15% of the capacity has been observed after 1,000 cycles in this range of potentials. For PC/1 M NEt_4BF_4, the capacitance is lower, probably due to a relatively high viscosity of the propylene carbonate [48], which limits the incorporation of the electrolyte into the pores of the nanocomposite. On the other hand, the cycling stability is largely improved in such an electrolyte by comparison with the electrolyte containing acetonitrile (or water).

Recently, many investigations have been carried out on the electroactive properties of materials for electrochemical storage using RTILs [48–51]. Due to their specific physical and chemical properties, RTILs can favorably replace classical liquid electrolytes. Indeed, they are nonvolatile, nonflammable, and have high ionic conductivity and a wide electrochemical window. They have been used in double-layer active carbon supercapacitors [49–52] and in conducting polymer-based supercapacitors [53–58].

Figure 6 shows the first results of the electroactivity of nanocomposites PPy/Fe_2O_3 in EMITFSI. During positive doping of the PPyPTS/Fe_2O_3, the capacity of the composite reaches 53 mAh/g, with a loss of only 4% after 1,000 cycles. The capacity is higher than that observed in PC/NEt_4BF_4, and the stability is largely improved in compar-

Table 4 Influence of the pore size distribution on the charge storage capacity

Samples	BET (m^2/g)	Pore size distribution				Q_{max} (mAh/g)
		<6 nm	6–20 nm	20–80 nm	>80 nm	
B	49	29.49	41.82	20.52	8.17	12
D3	45	8.62	18.84	38.03	34.52	47

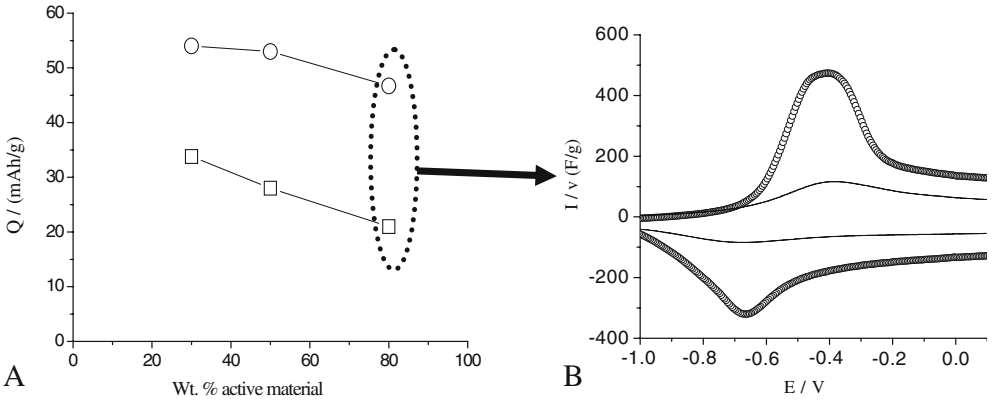

Fig. 5 Influence of the amount of active material in the electrode on the charge storage capacity for PPyPTS/Fe_2O_3 (sample D3) (*circle*) and for PPyPTS (sample C) (*square*) at 1 mV/s (**a**) and evolution of the capacitance vs voltage for 80 wt.% of nanocomposite D3 and PPyPTS in the electrode at 1 mV/s (**b**)

ison with CH_3CN/NEt_4BF_4 or $H_2O/LiClO_4$. Although the viscosity of the ionic liquid is quite high, the capacity of the nanocomposite is still high, probably due to the possibility to the molten salt to be incorporated into the pores of the nanostructured electrode. The coulombic reversibility is quantitative, which indicates a good electrochemical stability of the doped materials in this ionic liquid due to the large electrochemical window of this molten salt (4.3 V), which can limit secondary reactions during the oxidation of the nanocomposite.

Electrodes containing 80 wt.% in PPyPTS/Fe_2O_3 (D3) were studied in EMITFSI, and their electrochemical behavior (evolution of the capacitance vs potential) have been compared to PPyPTS (also at 80 wt.%). We observed, for the nanocomposites, a large contribution of the faradic process, which indicates a good charge transfer between the nanostructure and the molten salt. Probably due to the pore size distribution of the nanostructure, which is important enough to ensure the incorporation of anions inside the bulk of the electrode, the capacitance can reach 420 F/g (Fig. 7). By comparison, the electrode containing 80 wt.% of PPyPTS showed an important decrease of the capacitance limited to 156 F/g, and moreover, we did not see the presence of a well-defined peak (as observed for the nanocomposites), which would indicate a limitation of charge transfer in the material due to a poor incorporation of the RTIL in the bulk of the composite electrode and/or a low electronic percolation due to the low content of acetylene black in the material. As the highest content of ECP is needed in supercapacitor application, the realization of nanohybrid PPyPTS/Fe_2O_3 seems to be a good way to increase the charge storage capacity of electrodes.

Conclusions

Polymerization of pyrrole into a colloidal solution of Fe_2O_3 and in the presence of PTS anions improves the charge storage capacity of the material and has been attributed to a morphology modification of the composite. Nanoparticles act as a support to the polymerization process of pyrrole and lead to a more porous structure with a higher specific surface area, which increases the accessibility of the conducting polymer sites during the electrochemical process.

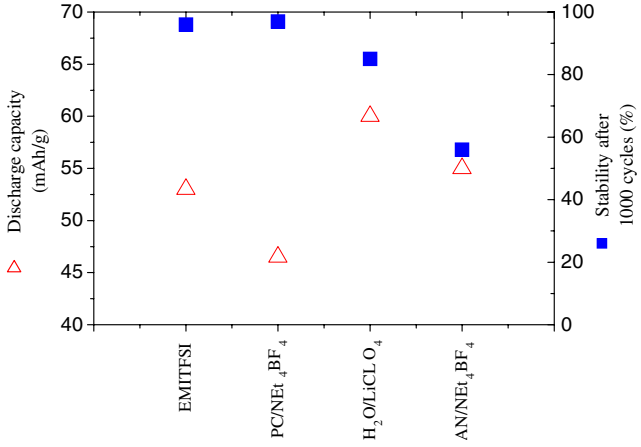

Fig. 6 Cyclability performance of PPyPTS/Fe_2O_3 (sample D3) at ±10 mA between −1.0 and 0.1 V vs $Ag:Ag^+$ for the organic electrolyte and vs SCE for the aqueous electrolyte

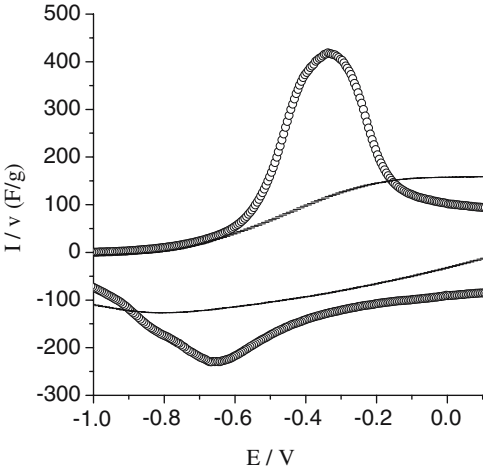

Fig. 7 Comparison of the capacitance vs voltage for 80 wt.% of PPyPTS/Fe_2O_3 (sample D3) (*circle*) and PPyPTS (*solid line*) electrodes at 1 mV/s in EMITFSI

Moreover, the kinetics of charge transfer is modified in this nanocomposite structure. The insertion–extraction of anions during the charge–discharge process is easier and allows for higher rates of charge–discharge. Higher power density is then expected. A high content of PPyPTS/Fe_2O_3 nanocomposites (80 wt.%) can be incorporated into an electrode whose performances are largely improved in comparison with similar electrodes containing PPyPTS.

Preliminary results indicate the promising influence of using a RTIL as electrolyte. Indeed, high capacitances and a good stability were obtained even for high content (80 wt. %) of electroactive nanomaterial in the electrode. The use of other RTILs and the syntheses of similar nanocomposites with polythiophene derivatives are actually in progress at our laboratory.

Acknowledgements The authors would like to thank the Agence de l'Environnement et de la Maîtrise de l'Energie for its financial support and P. Porte (research engineer) from Villetaneuse university for the BET measurements.

References

1. Rudge A, Davey J, Raistrick I, Gottesfeld S, Ferraris JP (1994) J Power Sources 47:89
2. Mastragostino M, Paraventi R, Zanelli A (2000) J Electrochem Soc 147:3167
3. Hannecart E, Destryker E, Fauvarque JF, Guibert AD, Andrieu X (1991) European Patent Application EP 413382 A1 19910220
4. Laforgue A, Simon P, Fauvarque JF, Mastragostino M, Soavi F, Sarrau JF, Lailler P, Conte M, Rossi E, Saguatti S (2003) J Electrochem Soc 150:A645
5. Talbi H, Just PE, Dao LH (2003) J Appl Electrochem 33:465
6. Hu CC, Li WY, Lin JY (2004) J Power Sources 137:152
7. Zhang QW, Zhou X, Yang HS (2004) J Power Sources 125:141
8. Frackowiak E, Béguin F (2002) Carbon 40:1775
9. Khomenko V, Frackowiak E, Beguin F (2005) Electrochim Acta 50:2499
10. Xiao Q, Zhou X (2003) Electrochim Acta 48:575
11. Hughes M, Shaffer MSP, Renouf AC, Singh C, Chen GZ, Fray DJ, Windle AH (2002) Adv Mater 14:382
12. Hughes M, Chen GZ, Shaffer MSP, Fray DJ, Windle AH (2002) Chem Mater 14:1610
13. An K, Hyeok J, Kwan K, Heo JK, Lim SC, Bae DJ, Lee YH (2002) J Electrochem Soc 149:A1058
14. Hashmi SA, Upadhyaya HM (2002) Ionics 8:272
15. Leroux F, Goward G, Power WP, Nazar LF (1997) J Electrochem Soc 144:3886
16. Kanatzidis MG, Tonge LM, Marks TJ, Marcy HO, Kannewurf CR (1987) J Am Chem Soc 109:3797
17. Arbizzani C, Balducci A, Mastragostino M, Rossi M, Soavi F (2003) J Power Sources 119:695
18. Kanatzidis MG, Marcy HO, McCarthy WJ, Kannewurrf CR, Marks TJ (1989) Solid State Ionics 32:594
19. He BL, Zhou YK, Zhou WJ, Dong B, Li HL (2004) Mater Sci Eng Abstr 374:322
20. Sanchez C, Ribot F (1994) New J Chem 18:1007 (Special issue)
21. Gangopadhyay R, De A (2000) Chem Mater 12:608
22. Murugan AV, Gopinath CS, Vijayamohanan K (2000) Electrochem Commun 7:213
23. Huguinin F, Girotto EM, Torresi RM, Buttry DA (2002) J Electroanal Chem 536:37
24. Sunderland K, Brunetti P, Spinu L, Fang J, Wang Z, Lu W (2004) Mater Lett 58:3136
25. Jarjayes O, Fries PH, Bidan G (1995) Synth Met 69:343
26. Deng J, Peng Y, He C, Long X, Li P, Chan ASC (2003) Polym Int 52:1182
27. Butterworth MD, Bell SA, Armes SP, Simpson AW (1996) J Colloid Interface Sci 183:91
28. Yang X, Xu L, Ng SC, Chan SOH (2003) Nanotechnology 14:624
29. Gangopadhyay R, De A (1999) Eur Polym J 35:1985
30. Chen A, Wang H, Li X (2004) Synth Met 145:153
31. Chen A, Wang H, Zhao B, Li X (2003) Synth Met 139:411
32. Chen W, Li X, Xue G, Wang Z, Zou W (2003) Appl Surf Sci 218:215
33. Murillo N, Ochoteco E, Alesanco Y, Pomposo JA, Rodriguez J, Gonzalez J, Del Val JJ, Gonzalez JM, Britel MR, Varela-Feria FM, De Arellano-Lopez AR (2004) Nanotechnology 15:S322
34. Suri K, Annapoorni S, Tandon RP, Mehra NC (2002) Synth Met 126:137
35. Maeda S, Armes SP (1995) Synth Met 73:151
36. Malinauskas A (2001) Polymer 42:3957
37. Caruso F (2001) Adv Mater 13:11
38. Gomez-Romero P (2001) Adv Mater 13:163
39. Chatterjee S, Sarkar S, Bhattacharyya SN (1993) J Photochem Photobiol A Chem 72:183
40. Bonhôte P, Dias AP, Papageorgiou N, Kalyanasundram K, Gratzel M (1996) J Inorg Chem 35:1168
41. Laforgue A, Simon P, Fauvarque JF (2001) Synth Met 123:311
42. Noh KA, Kim DW, Jin CS, Shin KH, Kin JH, Ko JM (2003) J Power Sources 124:593
43. Gangopadhyay R, De A, Das S (2000) J Appl Phys 87:2363
44. Ingram MD, Staesche H, Ryder KS (2004) Solid State Ionics 169:51
45. Ingram MD, Staesche H, Ryder KS (2004) J Power Sources 129:107
46. Naoi K, Oura Y, Maeda M, Nakamura S (1995) J Electrochem Soc 142:417
47. Suematsu S, Oura Y, Tsujimoto H, Kanno H, Naoi K (2000) Electrochim Acta 45:3813
48. Herlem G, Tran-Van P, Marque P, Fantini S, Penneau JF, Fays B, Herlem M (2002) J Power Sources 107:80
49. Ue M, Takeda M, Toriumi A, Kominato A, Hagiwara R, Ito Y (2003) J Electrochem Soc 150:A499
50. Frackowiak E, Lota G, Pernak J (2005) Appl Phys Lett 86:164104
51. Sato T, Masuda G, Takagi K (2004) Electrochim Acta 49:3603
52. Kim YJ, Matsuzawa Y, Ozaki S, Park KH, Kim C, Endo M, Yoshida H, Masuda G, Sato T, Dresselhaus MS (2005) J Electrochem Soc 152:A710
53. Stenger-Smith JD, Webber CK, Anderson N, Chafin AP, Zong K, Reynolds JR (2002) J Electrochem Soc 149:A973
54. Naudin E, Ho HA, Branchaud S, Breau L, Belanger D (2002) J Phys Chem B 106:10585
55. Randriamahazaka H, Plesse C, Teyssié D, Chevrot C (2003) Electrochem Commun 5:613
56. Randriamahazaka H, Plesse C, Teyssié D, Chevrot C (2005) Electrochim Acta 50:4222
57. Balducci A, Bardi U, Caporali S, Mastragostino M, Soavi F (2004) Electrochem Commun 6:566
58. Balducci A, Henderson WA, Mastragostino M, Passerini S, Simon P, Soavi F (2005) Electrochim Acta 50:2233